



Identification of a Glycosaminoglycan Binding Region of the Alpha C Protein That Mediates Entry of Group B Streptococci into Host Cells

Citation

Baron, Miriam J., David J. Filman, Gina A. Prophete, James M. Hogle, and Lawrence C. Madoff. 2007. "Identification of a Glycosaminoglycan Binding Region of the Alpha C Protein That Mediates Entry of Group B Streptococci into Host Cells." *Journal of Biological Chemistry* 282 (14): 10526–36. <https://doi.org/10.1074/jbc.m608279200>.

Published version

<https://doi.org/10.1074/jbc.M608279200>

Link

<http://nrs.harvard.edu/urn-3:HUL.InstRepos:41483179>

Terms of use

This article was downloaded from Harvard University's DASH repository, and is made available under the terms and conditions applicable to Other Posted Material (LAA), as set forth at

<https://harvardwiki.atlassian.net/wiki/external/NGY5NDE4ZjgzNTc5NDQzMGIzZWZhMGFIOWI2M2EwYTg>

Accessibility

<https://accessibility.huit.harvard.edu/digital-accessibility-policy>

Share Your Story

The Harvard community has made this article openly available. Please share how this access benefits you. [Submit a story](#)

Identification of a Glycosaminoglycan Binding Region of the Alpha C Protein That Mediates Entry of Group B *Streptococci* into Host Cells*

Received for publication, August 30, 2006, and in revised form, January 19, 2007. Published, JBC Papers in Press, January 26, 2007, DOI 10.1074/jbc.M608279200

Miriam J. Baron^{†1}, David J. Filman[§], Gina A. Prophete[‡], James M. Hogle[§], and Lawrence C. Madoff[‡]

From the [‡]Channing Laboratory, Department of Medicine, Brigham & Women's Hospital, and the [§]Department of Biological Chemistry & Molecular Pharmacology, Harvard Medical School, Boston, Massachusetts 02115

Group B *Streptococcus* (GBS) frequently colonizes the human gastrointestinal and gynecological tracts and less frequently causes deep tissue infections. The transition between colonization and infection depends upon the ability of the organism to cross epithelial barriers. The alpha C protein (ACP) on the surface of GBS contributes to this process. A virulence factor in mouse models of infection, and prototype for a family of Gram-positive bacterial surface proteins, ACP facilitates GBS entry into human cervical epithelial cells and movement across cell layers. ACP binds to host cell surface glycosaminoglycan (GAG). From crystallography, we have identified a cluster of basic residues (BR2) that is a putative GAG binding area in Domain 2, near the junction of the N-terminal domain of ACP and the first of a series of tandem amino acid repeats. D2-R, a protein construct including this region, binds to cells similarly to full-length ACP. We now demonstrate that the predicted charged BR2 residues confer GAG binding; site-directed mutagenesis of these residues (Arg¹⁷², Arg¹⁸⁵, or Lys¹⁹⁶) eliminates cell-binding activity of construct D2-R. In addition, we have constructed a GBS strain expressing a variant ACP with a charge-neutralizing substitution at residue 185. This strain enters host cells less effectively than does the wild-type strain and similarly to an ACP null mutant strain. The point mutant strain transcytoses similarly to the wild-type strain. These data indicate that GAG-binding activity underlies ACP-mediated cellular entry of GBS. GBS entry into host cells and transcytosis of host cells may occur by distinct mechanisms.

Group B *Streptococcus* (GBS)² is a common colonizer of human mucosal surfaces and causes invasive infections in

* This work was supported by National Institutes of Health Grants AI38424 (to L. C. M.) and AI059495 (to M. J. B.). The costs of publication of this article were defrayed in part by the payment of page charges. This article must therefore be hereby marked "advertisement" in accordance with 18 U.S.C. Section 1734 solely to indicate this fact.

The nucleotide sequence(s) reported in this paper has been submitted to the GenBank™/EBI Data Bank with accession number(s) M97256.

The amino acid sequence of this protein can be accessed through NCBI Protein Database under NCBI accession number AAA26848.

The atomic coordinates and structure factors (code 2O0I) have been deposited in the Protein Data Bank, Research Collaboratory for Structural Bioinformatics, Rutgers University, New Brunswick, NJ (<http://www.rcsb.org/>).

¹ To whom correspondence should be addressed: Channing Laboratory, 181 Longwood Ave., Boston, MA 02115. Tel.: 617-525-0752; Fax: 617-731-1541; E-mail: mbaron@partners.org.

² The abbreviations used are: GBS, group B *Streptococcus*; ACP, alpha C protein; GAG, glycosaminoglycan; BR2, binding region 2; Alp, alpha-like

neonates, peripartum women, and nonpregnant adults with underlying conditions. In these hosts, GBS virulence factors may promote infection by interacting with epithelial barriers in colonized sites, allowing penetration into deeper tissues.

Alpha C protein (ACP) is a GBS virulence factor that interacts with epithelial cells. ACP is expressed on many serotype Ia, Ib, and II strains and is the prototype for a family of proteins (alpha-like proteins, Alps) found on the surface of other GBS strains and of other Gram-positive organisms, such as the group A *Streptococcus* and enterococci. Alpha-like proteins share sequence homology and similar structural elements, including an N-terminal domain, a variable number of tandem repeats of ~80 amino acids each, and a C-terminal domain that includes a cell-wall anchor LPXTG motif common among Gram-positive species. Gene recombination within the repeat region leads to loss of repeats and allows variation in protein size; nonetheless, these proteins elicit protective antibody in mouse models of infection (1, 2). Deletion of the gene encoding ACP attenuates GBS virulence *in vivo*. In cell culture, the null mutant strain enters and transcytoses human cervical epithelial cells (ME180 cells) less effectively than does the wild-type parent strain. As a soluble protein construct, the N-terminal domain of ACP (NtACP) inhibits entry of wild-type GBS into these cells (3, 4).

GBS colonizes mucosal sites frequently but causes invasive disease relatively infrequently. The transition between colonization and invasive infection is not well understood. ACP may contribute to this process by promoting GBS entry into and transcytosis of host cells, but both the relationship between entry and transcytosis, and the mechanism(s) by which ACP facilitates these activities are unknown. Specifically, GBS may cross cell layers by an intracellular route and/or a paracellular route. Paracellular movement has been described for group A *Streptococcus* (5) and GBS (6). Intracellular GBS may transcytose into deeper tissues to cause invasive infection, or, instead, the epithelial cell containing intracellular GBS may be shed to protect the host from invasive infection, as described for *Pseudomonas aeruginosa* (7). The association of ACP with GBS internalization of epithelial cells *in vitro* (4) and the attenuated virulence of a GBS strain lacking ACP *in vivo* (3) support an association of GBS internalization of epithelial cells with inva-

protein; NtACP, N-terminal region of alpha C protein; erm, erythromycin; Bis-Tris, 2-[bis(2-hydroxyethyl)amino]-2-(hydroxymethyl)propane-1,3-diol; BSA, bovine serum albumin; PBS, phosphate-buffered saline; THB, Todd Hewitt broth.

sive illness. Better understanding of the interaction between ACP and its host cell receptor(s) on a molecular level will allow further studies addressing these and other questions.

Recombinant full-length ACP binds to heparin; ACP also binds cervical epithelial cell surface glycosaminoglycan (GAG) and enters these cells (8). In contrast, neither soluble NtACP nor soluble repeat region constructs mimic these behaviors. Structural data from crystallography studies of NtACP reveal two domains. Domain 1 (most distal from the bacterial surface), including Ser⁵⁷–Asp¹⁶⁰ with a predominant beta sheet structure, has a motif associated with integrin binding in other proteins. Domain 2 (connects distally to Domain 1 and proximally to the repeat region), including Ser¹⁶¹–Leu²²⁵, has a predominant α -helix structure. The surface amino acids of NtACP are mainly acidic (negatively charged), with the exception of two small clusters of positively charged residues (Fig. 1). The larger cluster (basic region 2, or BR2), located predominantly in Domain 2, includes several positively charged residues spaced on average 6 Å apart. This configuration of charged residues may confer GAG-binding activity by associating with sulfate groups on heparin. Of the charged residues of BR2 (Lys⁷², Lys⁹⁰, Arg¹⁶⁵, Lys¹⁹⁶, Arg¹⁷², and Arg¹⁸⁵), most are conserved (Lys⁷² in Domain 1 and Arg¹⁶⁵, Lys¹⁹⁶, and Arg¹⁸⁵ in Domain 2) or conserved by charge (Lys⁹⁰ in Domain 1) among all known alpha-like proteins. A construct (D2-R) including most of Domain 2, the region of NtACP lying closest to the junction with the repeat region, and one “repeat,” binds to heparin and host cell surface GAG similarly to full-length ACP (9). These data suggest that the GAG-binding region of ACP resides in this junctional region and includes BR2.

On the basis of these data, we hypothesized that the charged residues of BR2 bind to highly sulfated GAGs and that this GAG-binding activity is required for the described ACP-mediated effects in cell culture studies: internalization of GBS into host cells and transcytosis of host cells. We now report the results of our studies testing these hypotheses. We have found that desulfated GAGs do not inhibit ACP-host cell binding. We have altered the putative GAG-binding residues of NtACP in D2-R and found that these mutations diminish binding of soluble D2-R constructs to host cells. We have also designed a strain of GBS expressing a non-GAG-binding ACP variant. In a model of bacterial-epithelial cell interaction, this mutated strain enters host cells less well than the wild-type strain, whereas transcytosis rates are similar for the two strains. These data suggest GAG binding is required for ACP-mediated cellular entry of GBS. The mechanisms of GBS entry into host cells and transcytosis of host cells may be distinct.

EXPERIMENTAL PROCEDURES

Strains/Plasmids/Cells and Growth Conditions

GBS strain A909 is the prototype serotype Ia/C ($\{\alpha\}+$, $\{\beta\}+$) strain (10). A909 genomic DNA contains a copy of the *bca* gene encoding ACP (11). The strain was grown in Todd Hewitt broth (THB, Difco). *Escherichia coli* strain BL21(DE3) (Novagen) was used to express NtACP from pDEK14 (12), construct D2-R, and NtACP and D2-R mutant constructs; proteins were expressed and purified as described previously, via purifi-

cation over a histidine-binding nickel column (4, 9, 13). Mutant constructs were designed as described below, then expressed and purified similarly. Strain JL2054 is an ACP deletion mutant derived in the A909 background (3).

For homologous recombination work, GBS was grown in liquid culture in THB supplemented with yeast extract to 0.5% (w/v) (THY), on trypticase soy agar supplemented with 5% sheep blood (Becton-Dickinson, Cockeysville, MD), or on THY agar plates supplemented with antibiotics and 5% defibrinated sheep blood (PML Microbiologicals, Tualatin, OR). TOP10 *E. coli*-competent cells (Invitrogen) were used for cloning and grown in Luria-Bertani (LB) medium or on LB agar. When appropriate, the medium was supplemented with ampicillin at 100 μ g/ml or with erythromycin (*erm*) at 1 μ g/ml for GBS or 250 μ g/ml for *E. coli*. GBS was grown static in liquid culture as described previously (14). *E. coli* was grown with shaking at 37 °C. Plasmid pCR2.1 (Invitrogen) is an *E. coli* vector used for the direct cloning of PCR products; pJRS233 is a temperature-sensitive *E. coli*/Gram-positive shuttle vector (15).

ME180 (ATCC HTB33), a human cervical epithelial carcinoma cell line (ATCC), was propagated at 37 °C with 5% CO₂ in RPMI 1640 medium with L-glutamine, supplemented with 10% fetal calf serum and 1% penicillin-streptomycin (Invitrogen).

DNA Isolation and Manipulations

Plasmid DNA was isolated with the Qiagen Plasmid Maxi, Midi, or Mini Kit (Qiagen, Valencia, CA). GBS chromosomal DNA was prepared with the Qiagen DNeasy Tissue Kit. Restriction endonuclease digestions, DNA ligations, transformation of CaCl₂-competent *E. coli*, agarose gel electrophoresis, and Southern hybridizations (ECL, Amersham Biosciences) were performed by standard techniques (16). GBS electrocompetent cells were prepared as described (17) and transformed by electroporation with a Bio-Rad Gene Pulser II as described (18).

Site-directed Mutagenesis

Cloning of the DNA encoding the NtACP and D2-R constructs has been described previously (9, 12). These plasmids were used as templates for design and production of constructs containing site-directed mutations, in which Domain 2 residues Lys¹⁹⁶, Arg¹⁷², and Arg¹⁸⁵ were replaced with alanine residues using the QuikChange site-directed mutagenesis kit (Stratagene) according to the manufacturer's instructions. For Lys¹⁹⁶, forward primer Lys¹⁹⁶ F and reverse primer Lys¹⁹⁶ R were used; for Arg¹⁷², forward primer Arg¹⁷² F and reverse primer Arg¹⁷² R were used; and for Arg¹⁸⁵, forward primer Arg¹⁸⁵ F and reverse primer Arg¹⁸⁵ R were used (Table 1), generating plasmids pMG18, pMG17, and pMG13. Initially single site mutations were made; the process was repeated with these single site mutant plasmids used as templates for incorporating double site and triple site mutations. The constructs were transformed into *E. coli* strain BL21(DE3) for expression of the mutant forms of NtACP and D2-R. Histidine-tagged proteins were expressed and purified by nickel-affinity chromatography as described previously, using reagents from Novagen (4). Briefly, for each construct, a 2-liter culture of each *E. coli* transformant strain was rotated (200 rpm) at 37 °C to an A₆₀₀ equal to 0.6. Protein expression was induced with 1 mM isopropyl

TABLE 1
Primers used

Primer	Sequence
Lys ¹⁹⁶ F	5'-TGAGGTTTAAACAGGATTAGATACAATTGCAACAGATATGATAAATAATCCTAAGACGC-3'
Lys ¹⁹⁶ R	5'-CGGCTTAGGATTATATCAATATCTGTGCAATTGTATCTAATCCTGTTAAACCTCA-3'
Arg ¹⁷² F	5'-GAGGGATAAGATTGAAGAAGTTGCAACGAATGCAAACGATCCTAA-3'
Arg ¹⁷² R	5'-TTAGGATCGTTTGCATTTCGTTGCAACTTCTTCAATCTTATCCCTC-3'
Arg ¹⁸⁵ F	5'-CCTAAGTGGACGGAAGAAAGTGAACCTGAGGTTTAAACAGGATTAGA-3'
Arg ¹⁸⁵ R	5'-TCTAATCCTGTAAAACCTCAGTTGCACCTTCTTCCGTCCTACTTAGG-3'
N-term C6 Fwd HindIII	5'-AAGCTTTTGAGGGATAAGATT-3'
N-term C6 Rev BamHI	5'-GGATCCCAATACTAACAATTT-3'
1 rpt C6 Rev	5'-TTCCCTCCTGTTGGATCATA-3'
M13-20	5'-GTAAAACGACGGCCAG-3'
M13-Reverse	5'-CAGGAACAGCTATGAC-3'
D1 For	5'-CGCTAGCACAAATTCAGGGAGTGCAGCG-3'
D1 Rev	5'-TCAATTTTCGTTGTGATTGATATAG-3'

1-thio- β -D-galactopyranoside for 3 h at 37 °C rotating. The cells were harvested by centrifugation at 4000 \times *g* for 10 min at 4 °C, resuspended in 200 ml of Bind Buffer (5 mM imidazole, 0.5 M NaCl, 20 mM Tris-HCl, pH 7.9) containing 1% Protease Inhibitor Mixture Set III (Invitrogen), and lysed using a French pressure chamber. The lysate was centrifuged at 20,199 \times *g* for 20 min at 4 °C, and the supernatant was filtered using a 0.45- μ m sterile membrane. A 15-ml His-Bind resin (Novagen) column charged with 50 mM NiSO₄ was equilibrated in Bind Buffer, and the filtrate was loaded onto the column and allowed to pass through the resin by gravity flow. The column was washed with Wash Buffer (60 mM imidazole, 0.5 M NaCl, 20 mM Tris-HCl, pH 7.9) and eluted with Elute Buffer (1 M imidazole, 0.5 M NaCl, 20 mM Tris-HCl, pH 7.9). Fractions were collected and analyzed by SDS-PAGE using a 4–20% Tris-glycine gel (Cambrex) or 4–12% NuPAGE® Novex Bis-Tris gel (Invitrogen) under reducing conditions. Proteins were transferred to nitrocellulose for Western blotting. After blocking with 5% skim milk in phosphate-buffered saline containing 0.5% Tween 20 (PBT), the blots were allowed to react for 1 h with a 1:3,000 dilution (in PBT) of a monoclonal ACP-specific antibody (mouse ascites) (1). The blots were washed three times (5 min each) in PBT, then allowed to react with goat anti-mouse immunoglobulin G-alkaline phosphatase conjugate (Cappel, 1:3,000 dilution in PBT) for 1 h. The blots were again washed in PBT, equilibrated to pH 9.8, and then developed using 5-bromo-4-chloro-3-indolyl phosphate/nitro blue tetrazolium phosphatase substrate. These proteins were thus confirmed to bind to ACP-specific antibodies.

Flow Cytometry

Fluorescent Labeling of Proteins—An AlexaFluor-488 protein labeling kit (Molecular Probes) was used to conjugate AlexaFluor-488 dye to bovine serum albumin (BSA) and Alp products, according to the manufacturer's instructions. Calculations of the protein concentration and moles of label per mole of protein were performed based upon measurements of the *A*₂₈₀ and *A*₄₉₄ of the eluate, according to the manufacturer's instructions and as described previously (8).

Cell Staining—ME180 cells were grown to monolayer confluence in 6-well plates with 2 ml of RPMI 1640 with 10% fetal calf serum and 1% penicillin/streptomycin. Staining was performed as described (8). Briefly, the day prior to the assay, the medium was replaced with 1 ml of fresh medium, and the cells were incubated overnight at 37 °C with 5% CO₂. The next day 0.1 ml

of AlexaFluor 488-labeled 9-repeat ACP, N-terminal region, D2-R, mutant constructs, or BSA was added to the wells for a final concentration of 0.1 μ M. The 6-well plates were incubated at 37 °C with 5% CO₂ for 1.5 h. The medium was removed from the wells, and the monolayers were washed three times with 1 ml of PBS to remove nonadherent proteins. 350 μ l of trypsin-EDTA (0.25% trypsin, 1 mM EDTA-4Na, Invitrogen) was added to the wells, and the plates were incubated for 10 min at 37 °C. Cells were dislodged by repeat pipetting and harvested by centrifugation at 50 \times *g* (650 rpm) for 8 min. Cells were washed with 1 ml of PBS and resuspended in 0.1 ml of 2% paraformaldehyde in PBS at 4 °C overnight. The following morning, samples were washed with 1 ml of PBS to remove the fixative, resuspended in 0.4 ml of PBS, and filtered through a cell-strainer cap (Falcon), and at least 10,000 cells per sample were analyzed by flow cytometry (MoFlo, Cytomation). Data were plotted as cell count *versus* fluorescent intensity. The cell population of interest was determined by using the AlexaFluor 488-labeled BSA sample to define nonspecific fluorescence and/or autofluorescence levels; the positive staining region for the remaining samples was defined to include the highest 1–2% of cells stained in this BSA-stained sample.

For the inhibition studies, heparin sodium salt (Sigma-Aldrich, product H-3393), *N*-acetyl-de-*O*-sulfated heparin (Sigma-Aldrich, product A-6039), and de-*N*-sulfated heparin (Sigma-Aldrich, product D-4776) inhibitors were preincubated with labeled ACP at 4 °C for 1 h; mixtures were then added to the wells for an inhibitor concentration of 0–500 μ g/ml, and the mixture was incubated for 1.5 h at 37 °C. Cells were washed and analyzed by flow cytometry as above.

Crystallization

Preparations of wild-type and mutant NtACP proteins were prepared as described above. Crystals were grown at room temperature by hanging drop vapor diffusion (as reported previously for the wild-type protein (9)) over a well solution containing 0.1 M sodium acetate and 10% polyethylene glycol 4000, pH 5.0. Solutions of protein (at 17.24 mg/ml in 20 mM HEPES, pH 7.2) were mixed 1:1 with well solution just prior to crystallization.

A single crystal (>0.2 mm in each dimension) of the R185A mutant protein was mounted in a nylon loop, frozen by plunging into liquid nitrogen, and kept at 100 K in a nitrogen stream during data collection. Data were collected using CuK α radiation from an Elliott GX-13 rotating anode source, collected as a

TABLE 2
Data collection and refinement statistics

Data set	R185A
Space group	P6 ₂ 22
Unit cell (Å)	a = b = 55.7, c = 277.9
Resolution limits (Å)	20–3.1 (3.26–3.10) ^a
Total observations	92,814
Unique reflections	5,264
Redundancy	17.6
Completeness (%)	99 (99)
R_{merge}^c (%) ^b	14.3 (34.7)
R_{cryst}^c	24.7 (35.7)
R_{free}^c	26.8 (35.5)
Number of protein atoms	1,403
Ordered residues	57–236
Number of ions	0
Number of waters	0
Root mean square deviation bond length (Å)	0.011
Root mean square deviation bond angle (deg)	1.64

^a Values within parentheses are for the highest resolution shell.

^b $R_{\text{merge}} = \sum |I_h - \langle I_h \rangle| / \sum I_h$ over all h , where I_h is the intensity of reflection h .

^c R_{cryst} and $R_{\text{free}} = \sum |F_o| - |F_c| / \sum |F_o|$, where F_o and F_c are observed and calculated amplitudes, respectively. R_{free} was calculated using the 10% of data excluded from the refinement.

series of 165 1-degree oscillation images, recorded using a MAR 345-mm image plate detector, and processed using HKL-2000 (19).

Structure Determination and Refinement

The data set consisted of 92,814 measurements of 5,264 unique reflections in the range of 20- to 3.1-Å resolution (Table 2). Due to the high degree of redundancy in the data set, the unique reflections output were of acceptable quality.

Further processing of the data was done with CCP4 (20). A preliminary solution for the structure was obtained by molecular replacement, using MOLREP (21). This was done primarily to compensate for the tendency of the long c axis to vary from crystal to crystal. The input model consisted of the known structure of NtACP (PDB entry 1YWM), divided into two rigid bodies (residues 57–158 and 159–226, respectively), with the C-terminal His tag (residues 227–238) excluded, with a single overall temperature factor applied to the main-chain atoms. A second temperature factor, higher by 40, was applied to the side chains. The rigid body molecular replacement solution, calculated to 4.0-Å resolution, yielded an R -factor of 35.5, providing a preliminary indication that the mutant was folded in a native-like arrangement. This statistic was reduced to 29.5 by continuing rigid body refinement in REFMAC 5.2.0019 (22), adding a third body corresponding to the His tag, and with a temperature factor assigned to all side-chain atoms that was greater by 40.0 than that assigned to all main-chain atoms. Breaks in the main chain were then healed with an extremely brief (three cycle) refinement of all atoms.

Further rebuilding of the model in COOT (23), and refinement of the model, to 3.1-Å resolution, has yielded an R -factor of 24.7 with good geometry (Table 2). All main-chain torsions were within allowable limits. The cutoff for the refinement was $F > 0\sigma F$ (i.e. no cutoff was applied). The final model includes residues 57–225 of the ACP sequence, plus a linker and four histidines from the C-terminal His tag. The final model includes TLS parameters (24) and restrained individual temperature factors. The inclusion of fixed solvent molecules failed to improve upon R_{free} . Diffraction data and the refined model have been deposited in the Protein Data Bank (PDB ID 2O0I).

GBS Strain Expressing the ACP Variant

A strain of GBS expressing a variant ACP was derived by allelic exchange mutagenesis from wild-type strain A909 as described in a previous study (25), with modifications as follows.

Construction of Plasmid—The primers N-terminal C6 Fwd HindIII and N-terminal C6 Rev BamHI (designed to include restriction enzyme site sequences for BamHI and HindIII, respectively) were used to amplify D2-R, including the R185A mutation from plasmid pMG13. The resulting product was ligated into pCR2.1 (Invitrogen) and transformed into TOP10 *E. coli* cells (Invitrogen). The fragment of interest was isolated by digestion with BamHI and HindIII and ligated into plasmid pJRS233. The presence of the D2-R construct with R185A mutation was confirmed by DNA sequencing.

Transformants/Integrants—The R185A mutant construct in the temperature-sensitive shuttle vector pJRS233 was introduced into GBS strain A909 by electroporation. Transformants were selected by growth at 30 °C in the presence of *erm*. Cultures were serially passaged at 37 °C (non-permissive temperature) to select for integrants. Integration was confirmed by PCR using flanking primer pairs designed to include 1) an anticipated 300-bp fragment starting with plasmid DNA upstream of the D2-R mutant construct (M13–20) and ending with chromosomal DNA downstream of the mutant construct (1 rpt C6 Rev) and 2) an anticipated 600-bp fragment starting with chromosomal DNA upstream of the mutant construct (D1For) and ending with plasmid DNA downstream of the mutant construct (M13-Reverse). Integrants were further confirmed by Southern hybridization with HindIII-digested chromosomal DNA probed with the NtACP Domain 1 region (upstream of D2-R). The Domain 1 probe was generated by PCR amplification with D1 for and D1 rev primers (Table 1).

Excisants and Confirmation—Integrand strains were serially passaged in the absence of *erm*; excision of the plasmid from the chromosome via a second recombination event either completed the allelic exchange or reconstituted the wild-type genotype. *Erm*-sensitive colonies were screened for the expected mutation or reversion to wild-type Arg¹⁸⁵ by DNA sequencing of a fragment generated by PCR amplification with primer pair D1 For and N-terminal C6 Rev BamHI. HindIII-digested chromosomal DNA from excisants was probed with pJRS233 in Southern hybridization analysis to confirm loss of plasmid sequences from the mutant and revertant strains.

Characterization of Mutant and Revertant Strains—ACP expression was studied by Western blot: GBS strains A909 and JL2054 and R185A mutant were grown to $A_{650} = 0.7$ in THB at 37 °C. Bacteria were washed and resuspended in 20 μ l of PBS. Samples were run over SDS-PAGE and transferred to nitrocellulose and then probed with antibody specific for ACP (1) using the methods described above.

Growth Curves

Cultures were inoculated to $A_{650} = 0.03$ in THB and then incubated at 37 °C; the optical density was recorded every 20 min.

Capsule Extraction and Quantitation via Enzyme-linked Immunosorbent Assay Inhibition

These studies were performed as described (25). Briefly, 100-ml cultures of GBS strains A909 and R185A were grown to A_{650} 0.6 at 37 °C. Cultures were divided in half; 50 ml was centrifuged, and bacterial pellets were washed with PBS, then resuspended in 1 ml of protoplast buffer (30 mM NaHPO₄, 40% sucrose (w/v), 10 mM MgCl₂) with 1000 units of mutanolysin (Sigma-Aldrich) and incubated at 37 °C for 6 h to release polysaccharide from cells. Protoplasts were then removed by centrifugation at 3800 × *g* for 15 min. The amount of polysaccharide in the extract was determined using serial dilutions of the extract in a competition enzyme-linked immunosorbent assay, in comparison with a standard curve generated with purified type Ia capsular polysaccharide (kind gift of Dr. Dennis Kasper). The other half of the 100-ml culture was centrifuged, washed with PBS, and dried to determine the mass of GBS present. The assay was performed in duplicate. Results are expressed as milligrams of polysaccharide per gram of GBS. Means were compared using a *t* test.

GBS Internalization Studies

These experiments were performed as described (4); briefly, GBS were added to confluent ME180 cells in a 24-well plate. After 2 h at 37 °C, wells were washed with PBS to removed non-adherent bacteria and then treated with penicillin and gentamicin to kill the remaining extracellular bacteria. Cells were then washed and lysed. Lysate dilutions were plated to enumerate intracellular bacteria. The mean proportion of internalized bacteria was log-transformed, and strain-specific means were compared by mixed effects analysis of variance, allowing a fixed effect of strain and a random assay effect. Results are converted back to ratios on the raw scale (-fold differences) for presentation.

GBS Transcytosis Studies

These experiments were performed as described (4); briefly, GBS were added to ME180 cells grown to confluence on Transwells suspended in 12-well plate wells. At 1-h intervals, Transwells were moved to fresh wells, and the medium remaining in the lower chamber was serially diluted and plated to allow enumeration of transcytosed GBS. The mean number of transcytosed bacteria was log-transformed, and strain-specific means were compared by two-tailed Student's *t* test.

RESULTS

On the basis of our prior work suggesting binding of ACP to GAG, as well as other GAG-binding protein studies in which charged amino acid residues contribute significantly to GAG-binding interactions (26, 27), we hypothesized that charge interactions between sulfated GAGs and ACP residues mediate the binding of GAG to ACP. We tested this hypothesis by comparing the effect of desulfated heparin variants (Sigma-Aldrich) with the effect of fully sulfated heparin sodium (Sigma-Aldrich) on the binding of ACP to ME180 human cervical cells, because we had found previously that soluble heparin sodium interferes with the binding of ACP to these cells. In support of this

hypothesis, these soluble de-sulfated heparins do not inhibit ACP binding to ME180 cells. Specifically, in the absence of inhibitors, flow cytometry analysis shows that labeled ACP binds to 78.2% of cells. In the presence of 500 μM soluble heparin sodium, ACP binds 8.6% of cells (89% of baseline ACP binding is inhibited), whereas in the presence of the same concentrations of desulfated heparins, ACP binds 78.6% (de-*O*-sulfated heparin) or 85.6% (de-*N*-sulfated heparin) of cells (0% of baseline ACP binding is inhibited). These data indicate that, in contrast to heparin sodium, de-sulfated heparins do not inhibit the binding of ACP to host cells.

The high resolution structure of NtACP (9) allowed prediction of a GAG-binding domain BR2, including basic residues Lys⁷² and Lys⁹⁰ from the Domain 1 region of NtACP and Arg¹⁶⁵, Lys¹⁹⁶, Arg¹⁷², and Arg¹⁸⁵ in the Domain 2 region of NtACP (Fig. 1). Although no detailed structure of the repeat region is known, cell binding studies indicating involvement of an epitope spanning NtACP and the repeat region suggest the GAG-binding region of ACP may extend from Domain 2, the region of NtACP lying closest to the junction with the repeat region, into the repeat region. In support of this hypothesis is our report that D2-R (a portion of ACP, including approximately one-third of the NtACP (*i.e.* Leu¹⁶⁴–Leu²²⁵, most of Domain 2), and an adjacent repeat) maintains the GAG-binding activity of full-length ACP, binding to heparin in dot blot assays and to ME180 cervical cells. Soluble heparin inhibited the cell-binding activity in a concentration-dependent manner, as did full-length ACP (9). The following studies were performed to assess the contribution of the predicted charged Domain 2 residues to the GAG-binding activity of ACP.

Replacement of the Predicted GAG-binding Residues of Domain 2 Eliminates D2-R Binding to Cells

To identify BR2 residues (Fig. 1) contributing to GAG binding by D2-R, we used site-directed mutagenesis to construct variant proteins in which charged residues Arg¹⁷², Arg¹⁸⁵, and Lys¹⁹⁶ were replaced with neutral alanine residues. The plasmids were sequenced to confirm incorporation of the desired mutations with intact sequence in the rest of the construct. Purity was assessed (to be >90%) on Coomassie-stained gel. Western blots confirmed recognition of mutant proteins by ACP-specific antibodies (Fig. 2). Protein constructs were fluorescently labeled and incubated with ME180 cells. Flow cytometry revealed markedly lower levels of cell binding for the single site, double site, and triple site mutation constructs than for the native D2-R construct (Fig. 3). Specifically, labeled BSA (negative control) bound 1% of cells, whereas constructs D2-R, D2-R/R185A, D2-R/R172A, and D2-R/K196A bound 63.1%, 7.4%, 8.5%, and 4.3% of cells, respectively.

Mutations in the Predicted GAG-binding Residues of Domain 2 Do Not Alter Overall Protein Structure

We performed crystallization experiments to verify that mutations of the predicted GAG-binding residues of Domain 2 would not prevent proper folding of the protein and to help to verify the identity of the mutated residue. For these studies, we used site-directed mutagenesis to make variant protein con-

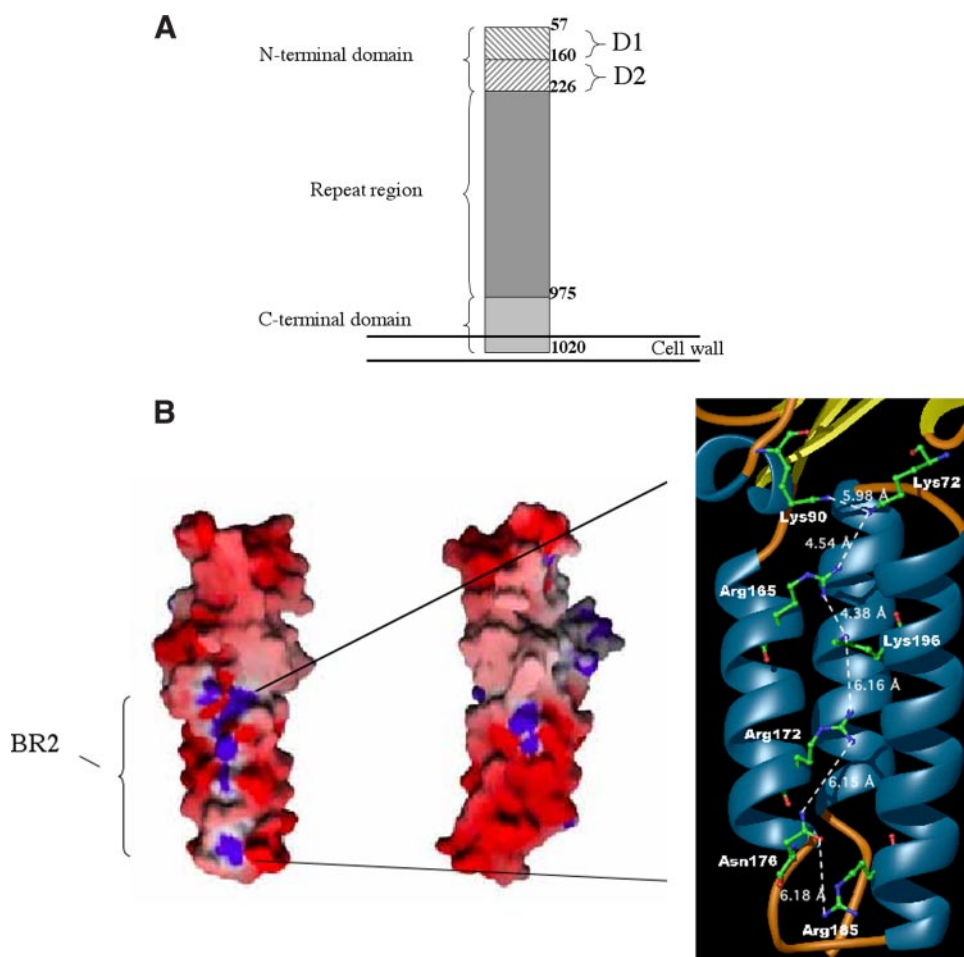


FIGURE 1. BR2, putative GAG-binding region of NtACP. *A*, schematic representation of the full-length ACP, including orientation of N-terminal domain (NtACP), repeat region, and C-terminal domain. The NtACP includes Domains 1 and 2 (*D1* and *D2*). *B*, molecular surface representation (GRASP (46)) derived from crystallography (PDB entry 1YWMM) of NtACP (9) showing a series of positively charged (blue) residues (*BR2*), constituting a putative heparin-binding domain. The views are related by a rotation of 180° around the vertical axis. *Inset*: detailed relationship of pocket residues (in order of increasing proximity to the repeat region) Lys⁷², Lys⁹⁰, Arg¹⁶⁵, Lys¹⁹⁶, Arg¹⁷², Asn¹⁷⁶, and Arg¹⁸⁵, hypothesized to contribute to binding to host cell surface GAG. Lys⁷², Arg¹⁶⁵, Arg¹⁸⁵, and Lys¹⁹⁶ are highly conserved among Alps. Construct D2-R, which retains GAG-binding activity, includes all these residues except Lys⁷² and Lys⁹⁰.

structures of NtACP in which charged residues Arg¹⁸⁵, Arg¹⁷², and Lys¹⁹⁶ were replaced with neutral alanine residues. We hypothesized that the overall structural integrity of these constructs was maintained because: 1) they were easily purified using the same protocols as those used for the wild-type protein, 2) they were stable over the long term (months), and 3) they maintained recognition by antibodies raised against the wild-type protein.

We chose the R185A construct for further study because structural data predict this residue lies closest to the junction of NtACP with the repeat region (9); both the NtACP and the repeat region are required for heparin binding (8). In addition, of the three mutation sites, only the Arg¹⁸⁵ side chain interacts with the main chain in the native NtACP crystal structure and appears to stabilize it, raising concern that mutation of this residue might lead to protein misfolding. We have less reason to be suspicious about the folding of the other two single site (172 and 196) mutants: neither of those two side chains made intramolecular contacts in the native crystal structure; both are entirely solvent-exposed, and both come from the middle of

their respective β strands, where strand termination is not an issue (9).

We crystallized the histidine-tagged protein expressed from this construct under similar conditions to those that allow crystallization of native NtACP (9) and collected diffraction data, generating data that scaled well to the structure factors of the wild-type NtACP construct ($R_{\text{cryst}} = 24.4$). These data indicate that the structure of the mutant is very similar to that of the native protein (0.50-Å root mean square deviation in the main chain).

A “difference map” allowed us to determine the differences between the wild-type and mutant construct data (Table 2 and Fig. 4). The lack of difference signal in the model aside from the R185A mutation site confirms that the mutation did not perturb the structure significantly, even locally near the R185A mutation. To provide a sensitive and only minimally biased indication that the mutated arginine side chain was indeed missing, a model-phased difference map was calculated, taking the Fourier amplitudes to be the difference between the present (mutant) data set (PDB entry 2O0I) and the resolution-scaled native data (PDB entry 1YWMM). Resolution-dependent scale factors for the native data set were calculated using a continuously sliding window, 200

reflections wide, in SFTOOLS.³ At a contour of 4.0 standard deviations above the mean, the only large peaks visible in the difference maps are negative, corresponding to the loss of the arginine side chain and minimal shifts in the main chain to which the guanidinium group was bound in the native structure (Fig. 4, orange contour). In corresponding F_o or $2F_o - F_c$ maps, the arginine side chain is indeed missing (Fig. 4, green contour).

Derivation of GBS Strain Expressing Variant ACP

To assess the importance of ACP GAG-binding activity in the interaction of live GBS with host cells, we derived a mutant strain from type Ia GBS strain A909. The mutant strain expresses a variant of ACP with R185A, in which Arg¹⁸⁵ is replaced by a neutral alanine residue. Of the putative GAG-binding site residues in Domain 2, Arg¹⁸⁵ is closest to the junction of NtACP with the repeat region; we thus hypothesized that charge replacement at this site would be most likely to interfere with GAG binding of the NtACP-repeat region

³ B. Hazes, unpublished results.

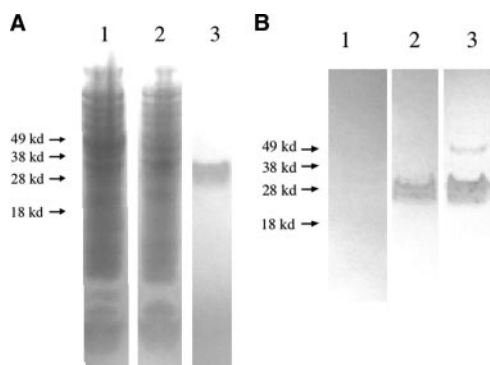


FIGURE 2. Nickel column-purified mutant D2-R protein is >90% pure and recognizes ACP-specific antibodies. Histidine-tagged protein construct D2-R with R185A was generated using site-directed mutagenesis. The protein was overexpressed in *E. coli*, and then purified over a nickel column; expected size is ~25 kDa. *A*, purified recombinant protein (lane 3) was run over SDS-PAGE (4–12% NuPAGE® Novex Bis-Tris gel (Invitrogen)) under reducing conditions and visualized with Coomassie staining along with controls: *E. coli* without plasmid (lane 1) and cells expressing recombinant protein prior to purification (lane 2). Purity was estimated to be >90%. *B*, samples were transferred to nitrocellulose for Western blotting and found to bind to ACP-specific antibodies: after blocking with 5% skim milk in phosphate-buffered saline containing 0.5% Tween 20 (PBT), the blots were allowed to react for 1 h with a 1:3000 dilution (in PBT) of a monoclonal ACP-specific antibody (mouse ascites) (1). The blots were washed three times (5 min each) in PBT, then allowed to react with goat anti-mouse immunoglobulin G-alkaline phosphatase conjugate (Cappel, 1:3000 dilution in PBT) for 1 h. The blots were again washed in PBT, equilibrated to pH 9.8, and then developed using 5-bromo-4-chloro-3-indolyl phosphate/nitro blue tetrazolium phosphatase substrate. Lane 1, *E. coli* without plasmid; lane 2, *E. coli* expressing recombinant protein prior to purification; lane 3, purified recombinant D2-R with R185A mutation.

junction. In support of this hypothesis, a soluble D2-R construct with this mutation interacted minimally with ME180 cells (9).

Confirmation of Integration—Plasmid pJRS233 (containing the *erm* resistance gene), including an insert encoding the Domain 2 region of NtACP with the R185A mutation was prepared and introduced into competent GBS strain A909 by electroporation. Transformants were selected with *erm*, and a plasmid was allowed to integrate into the chromosome. Integration was confirmed by PCR amplification with primers flanking the insert in the chromosome that showed 300- and 600-bp amplicons as expected, as well as by Southern hybridization analysis (Fig. 5A).

Characterization of Excisants—Integrants were passaged in broth to allow excision and loss of the pJRS233 plasmid. PCR amplicons of the area of interest from excisants (*erm*-sensitive colonies) were sequenced and classified as mutants (including R185A mutation) or revertants (wild-type sequence). In addition, HindIII-digested chromosomal DNA from excisants was probed with pJRS233 in Southern hybridization analysis to confirm loss of plasmid sequences from the mutant and revertant strains (Fig. 5B). The mutant and revertant strains were compared with parent strain A909 and with null mutant strain JL2054 and had a similar growth rate. The mutant strain and parent strain A909 expressed similar levels of ACP by Western blot (Fig. 5C) and similar levels of polysaccharide capsule by enzyme-linked immunosorbent assay inhibition assay (mean \pm S.D. A909: 11.3 \pm 2.26 mg of capsule/g of GBS; R185A: 16.6 \pm 7.35 mg of capsule/g of GBS, $p = 0.2193$).

Variant ACP-expressing GBS Strain Enters Cells Less Effectively than Does Wild-type GBS

We studied the effects of the ACP GAG-binding mutation in the interaction of live GBS with ME180 cells in culture. Previously the A909 wild-type strain was reported to enter ME180 cells ~3-fold more effectively than a null mutant strain lacking the *bca* gene (4). Because we hypothesized that GAG binding mediates the ACP-associated entry into host cells, we anticipated that our GAG-binding site mutant strain R185A would internalize less well than the wild-type strain. To test this hypothesis, we incubated the parent strain (A909), null mutant (JL2054), and R185A mutant with host cells for 2 h as described before (4). We calculated the numbers of cell-associated (surface-bound and internalized) and internalized-only GBS in six separate repetitions of the experiments and analyzed as follows. The distribution of percent internalized was found to be in symmetry and approximately variance-stabilized across strains after application of \log_{10} transformation to the data from six independent assays. Mixed effects analysis of variance was applied to the \log_{10} transformed percent internalized results, allowing a fixed effect of strain and a random assay effect (28). The number of cell-associated GBS was similar for all GBS strains (data not shown). The cellular internalization of the revertant strain was statistically indistinguishable from that of the wild-type A909 strain ($p = 0.53$). The cellular internalization of the R185A mutant strain was statistically indistinguishable from that of the null mutant ($p = 0.35$). The wild-type strain A909 internalized four times as efficiently as the R185A mutant strain ($p = 0.0007$ versus ratio of 1). Thus the R185A mutation confers GBS internalization activity similar to that of the null mutant (4) (Fig. 6).

In contrast to these results in assays of internalization, in five independent experiments assaying transcellular movement, we noted no difference in rates of transcytosis of ME180 cells for the A909 versus the R185A mutant strain (mean log colony-forming units/ml 5.58 versus 4.75 at 3 h, $p = 0.27$; mean log colony-forming units/ml 6.11 versus 6.19 at 4 h, $p = 0.08$).

DISCUSSION

The interactions between GBS and epithelial cells are fundamental to the organism's relationships with its host both as colonizer and pathogen. The factors promoting one or the other of these outcomes are incompletely understood, and the mechanism and route of bacterial movement across epithelial surfaces in invasive infection are not clear. It is clear, however, that components of both the bacterial and host cell surfaces contribute to these events.

Various GBS surface components, including capsular polysaccharide (29), lipoteichoic acid (30), and surface proteins (ACP (4, 8), β -hemolysin/cytolysin (31), Spb1 (32), FbsA (33), FbsB (34), and SCPB/C5a peptidase (35), and GBS1478 (36)), contribute to host cell adhesion and internalization of GBS. FbsA and FbsB bind to fibrinogen, whereas structural features suggest that SCPB/C5a peptidase binds to host cell integrins (37).

Among these GBS surface entities, only ACP is reported to bind to host cell GAG. The involvement of host cell GAG in the

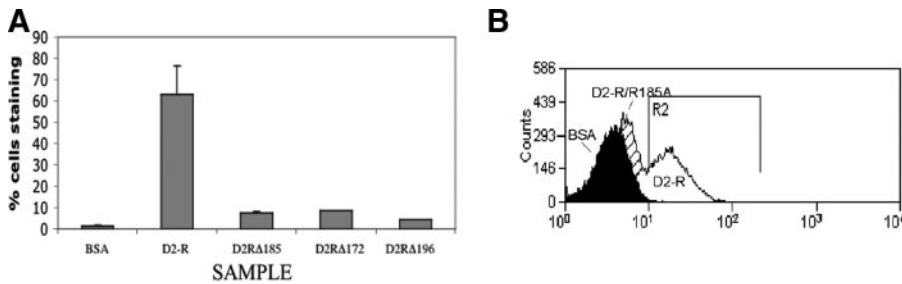


FIGURE 3. Site-directed mutagenesis of putative GAG-binding residues of D2-R markedly reduces association with human cervical cells. Confluent ME180 human cervical epithelial cells were incubated with AlexaFluor-488-labeled wild-type D2-R or mutant D2-R constructs in which residues Arg¹⁸⁵, Arg¹⁷², or Lys¹⁹⁶ were replaced with neutral alanines. Cells were then washed and analyzed by flow cytometry. Additional samples were incubated with labeled BSA. *A*, data (percentage of cells stained) show a reduction in binding by >80% for all single site mutants as compared with wild-type D2-R, despite lower efficiency of fluorescent labeling for the wild-type protein (0.89 mol of dye per mole of protein for wild-type versus 1.06–1.51 for single site mutant constructs). Similarly, double and triple site mutation constructs bound minimally to cells (data not shown). *B*, a representative histogram plot from one experiment is shown, expressed as cell count (*y*-axis) versus fluorescent intensity (*x*-axis), and R2 represents the region defined to be positive cell staining. These data reveal a shift in the peak representing staining cells for samples incubated with mutant D2-R compared with those incubated with wild-type D2-R. In this experiment, BSA (shaded region) bound 1.04% of cells, wild-type D2-R (open region) bound 72.4% of cells, and D2-R/R185A (hatched region) bound 5.03% of cells.

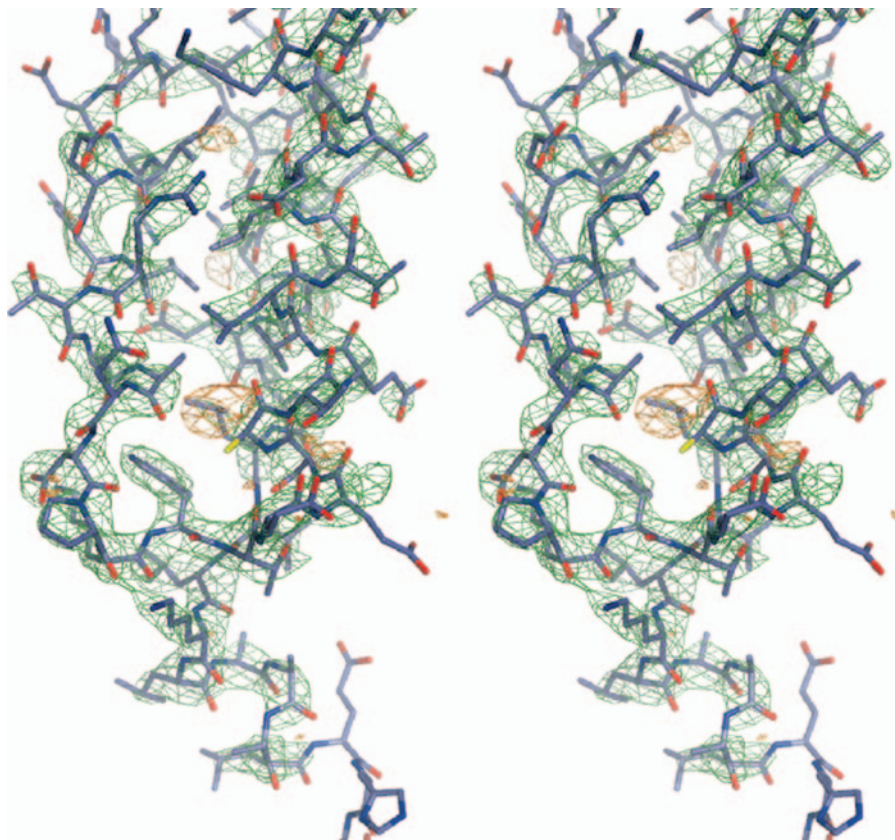


FIGURE 4. R185A mutation does not alter protein folding. Electron density features in the vicinity of the R185A mutation site. This stereo view shows the lower portion of Domain 2 of the NtACP mutant. The β carbon of Ala¹⁸⁵ is highlighted in yellow. The green wire frame represents an isocontour surface of the $2F_o - F_c$ electron density map. The orange wire frame shows a negative difference electron density contour (F mutant - F native, phased on the omit model) at 4 S.D. above the mean. Electron density belonging to neighboring molecules has been truncated for clarity. Electron density figure was prepared using PYMOL (DeLano Scientific LLC, San Carlos, CA).

pathogenesis of other organisms, including bacteria, viruses, mycobacteria, parasites, and prions, is well documented, and the contributions of the pathogen-host cell GAG interaction include promotion of adhesion (38), internalization (39), and

might be a co-receptor, and that mutations interfering with GAG binding thus might not entirely eliminate the ability of ACP to interact with host cells. Because of the contributions of non-ACP factors (described above) to internalization and tran-

scytosis (40). Earlier work indicating that ACP binds host cell GAG and promotes GBS internalization, and transcytosis of host cells led us to hypothesize that GAG-binding activity mediates these events.

Structural features of GAG-binding proteins have been described, based on correlation of structure-function analysis using site-directed mutagenesis in such systems as heparin-thrombin binding (26), heparin-fibroblast growth factor binding (27, 41), and heparin-viral protein binding (42). Some of these studies report the effects of mutations in the GAG-binding site on protein structure. On the basis of these studies, crystallography studies of NtACP, and our data showing enhanced GAG-binding activity of D2-R as compared with NtACP or repeat region alone, we identified a putative GAG binding region BR2 in Domain 2 of NtACP that likely extends into the repeat region.

Here we describe studies indicating that sulfated heparins inhibit D2-R binding to cellular GAG but desulfated heparins do not. These data support the hypothesis that GAG sulfate groups are required for the cellular interactions of ACP and more specifically, that positively charged residues in BR2 are required for the ACP-sulfate interaction, and that replacement of these residues reduces GAG binding and subsequent events that depend on GAG binding. On the basis of prior work showing that ACP promotes GBS entry into and transcytosis across human cervical epithelial cells, we hypothesized that neutral residue substitution of positively charged residues of BR2 would diminish GAG-binding activity of ACP and thus diminish the rates of ACP-mediated GBS entry and transcytosis of host cells. Because structural data also revealed a putative integrin-binding site in Domain 1 of NtACP, we hypothesized that host cell GAG

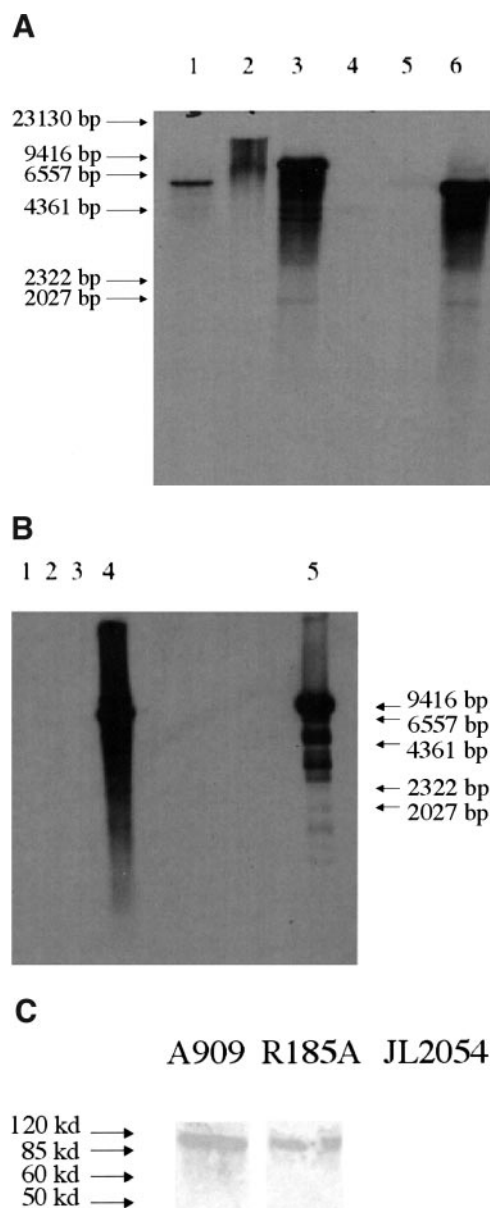


FIGURE 5. Derivation of a strain of GBS expressing variant version of ACP including GAG-binding site mutation R185A. *A*, integration of plasmid pJRS233/R185A in the A909 chromosome was confirmed with Southern blot hybridization: genomic DNA from strains A909, pJRS233/R185A transformant, and pJRS233/R185A integrant was digested with HindIII and run on 1% agarose gel. Probing with Domain 1, a region of NtACP upstream of the anticipated recombination site, results in a 6-kb fragment from wild-type A909 genomic DNA (lane 1) and the transformant (lane 6). Proper integration of the pJRS233/R185A construct enlarges the expected size of the fragment to 8.5 kb, seen in the integrant (lane 3). Lanes 2, 4, and 5 show uncut integrant DNA, uncut pJRS233/R185A plasmid, and HindIII-digested plasmid, respectively. *B*, loss of pJRS233 plasmid from excisants was confirmed with Southern blot hybridization: HindIII-digested chromosomal DNA from A909 (lane 1), A909/R185A (mutant, lane 2) and A909/R185R (revertant, lane 3), A909/pJRS233/R185A (integrant, lane 4), and pJRS233 (plasmid, lane 5) was probed with pJRS233 and revealed the absence of plasmid in the derived mutant and revertant strains. *C*, intact expression of ACP in the mutant strain (R185A) relative to the parent wild-type strain (A909) was confirmed by Western blot, probing with ACP-specific antibodies: GBS were grown to $A_{650} = 0.7$ in THB at 37 °C. Bacteria were washed and resuspended in 20 μ l of PBS. Samples were run over SDS-PAGE and transferred to nitrocellulose and then probed with antibody specific for ACP (1) using the methods described above. After blocking with 5% skim milk in phosphate-buffered saline containing 0.5% Tween 20 (PBT), the blots were allowed to react for 1 h with a 1:3000 dilution (in PBT) of a monoclonal ACP-specific antibody (mouse ascites) (1). The blots were washed three times (5 min each) in PBT, then allowed to react with goat

scytosis, we also anticipated that the effects of our mutations on overall internalization and transcytosis might be modest, similar to those of the null mutant strain JL2054.

Our data support these hypotheses, in that substitution of any of three charged residues in D2-R by alanine (sites 185, 172, or 196) eliminated binding of the protein to host cells *in vitro* without altering the folded protein structure in crystallization studies.

Further, a strain of GBS expressing ACP with the neutral substitution for Arg¹⁸⁵ entered host cells less efficiently than did the wild-type strain, acting like a null mutant strain completely lacking the gene for ACP. Interestingly, we found no difference between wild-type and R185A mutant strains in transcytosis assays. These data suggest that the GAG-binding region of ACP is required for ACP-mediated cellular entry but not for transcytosis of GBS.

These findings are of interest from several perspectives. First, they reveal that we have identified residues critical for GAG-binding activity in ACP and confirm the validity of the structure-function relationship predicted by the crystallographic structure of NtACP, in the contexts of full-length protein and of expression on the surface of GBS.

We hypothesized that residue 185, conserved among alpha-like proteins and predicted to lie most closely to the junction of NtACP with the repeat region, would be most essential to the GAG-binding activity we had mapped previously to this region, and our data support this hypothesis. However, it is interesting and not entirely expected that each single site mutation (172, 185, and 196) in D2-R leads to a similarly low level of cell-association compared with native protein. Although mutation of these charged residues might in theory lead to less efficient fluorescent labeling (as the labeling involves reaction of the succinimidyl ester of AlexaFluor-488 carboxylic acid with protein amines), which could make protein binding appear less efficient and explain our assay results, our calculations of labeling efficiency indicate this is not the case. In fact, the mutant proteins labeled slightly more efficiently than the wild-type protein. Another explanation for our findings is that a critical amount of positive charge within BR2 is necessary for binding, so that loss of any single charged residue results in a loss of adequate charge-mediated binding affinity with GAG. Several of our studies support this explanation: first, our finding that soluble desulfated GAG structures, unlike soluble sulfated GAG structures, do not impair binding of ACP to host cells, and second, our observation of similar cell-binding activity for constructs with replacement of charged residues regardless of whether these residues are conserved (residues 185 and 196) or not (residue 172) among alpha-like proteins. Because Domain 1 BR2 residues Lys⁷² and Lys⁹⁰ (Fig. 1) are absent from wild-type D2-R, our data raise the possibility that loss of any additional charged residue reduces GAG binding of D2-R.

anti-mouse immunoglobulin G-alkaline phosphatase conjugate (Cappel, 1:3000 dilution in PBT) for 1 h. The blots were again washed in PBT, equilibrated to pH 9.8, and then developed using 5-bromo-4-chloro-3-indolyl phosphate/nitro blue tetrazolium phosphatase substrate. A909 and the mutant strain (R185A) express ACP, whereas the null mutant strain, JL2054, lacks ACP expression.

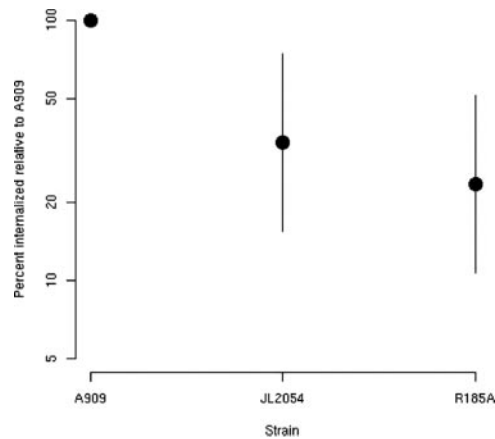


FIGURE 6. GBS strain R185A enters ME180 cells less effectively than does wild-type GBS strain A909. GBS strains A909, JL2054 (null mutant for ACP, previously shown to have diminished cell entry relative to A909), and R185A (point mutant in site associated with GAG-binding activity) were incubated with confluent ME180 cells at 37 °C for 2 h. Non-adherent GBS were washed away, and externally adherent GBS were killed with penicillin/gentamicin before cells were lysed and plated to enumerate internalized GBS. The percentages of internalized A909 and internalized mutant GBS relative to their starting inocula were calculated (% internalized). The mean proportion of internalized bacteria was log-transformed, and strain-specific means were compared by mixed effects analysis of variance, allowing a fixed effect of strain and a random assay effect. Results are converted back to ratios on the raw scale (-fold differences) for presentation. To facilitate comparison of strain performances in this assay, for each repetition of the experiment, the mutant strains' % internalized were normalized relative to the wild-type (A909) strain's % internalized in the same day's study. Data are shown as percentage of bacteria internalized relative to values for wild-type strain A909 (defined to be 100%), averaged from six separate repetitions of the experiment. The wild-type strain A909 internalized four times as efficiently as the R185A mutant strain ($p = 0.0007$ versus ratio of 1). The cellular internalization of the R185A mutant strain was statistically indistinguishable from that of the null mutant ($p = 0.35$).

Second, we constructed a strain of GBS that bears a GAG binding-deficient ACP variant but preserves binding to ACP-specific antibodies, bacterial growth rate, and capsule production, suggesting the differences in behavior of our mutant strain compared with the wild-type strain are specific to the point mutation R185A. The conservation of this residue among all known alpha-like proteins further suggests that this charged amino acid performs an important role in the biology of all proteins in this family. On this basis, our findings in studying the behavior of this mutant strain likely apply to other Alp-bearing bacteria also.

Third, this fairly subtle change in amino acid sequence influences the ability of the protein to interact with its binding partner(s) and mediate subsequent events, including cell internalization. These data suggest that GAG-binding activity is required for ACP-mediated entry of GBS into host cells. We have reported that ACP binding/entry into host cells is actin-dependent (8); thus this process may involve a host cell proteoglycan, a protein core anchoring GAG in the host cell membrane that may interact with the actin cytoskeleton to promote GBS uptake. Internalization may also involve a co-receptor, such as an integrin, as described in other systems (43, 44).

Finally, our data indicate that GAG binding may underlie some but not all recognized functions of ACP in interactions of GBS with host cells. Previous studies (4) show a role for ACP in both entry of GBS into ME180 human cervical cells and transcytosis of these cells. If entry and transcytosis occur via the

same mechanism, we would expect that a mutation affecting one process should also affect the other. We now report results from studies of GBS strain R185A, in which a charge-neutralizing mutation in residue 185 of the putative GAG-binding region of ACP is associated with diminished entry into host cells compared with the wild-type strain, whereas the rate of transcytosis is not affected by this mutation. These data suggest the two processes occur by distinct mechanisms and that the GAG binding of ACP may not be required for transcytosis. For example, ACP may mediate transcytosis by binding to a different receptor from that involved in cell entry, or transcytosis may occur after binding of the same receptor as entry, but with different affinity. Our results suggest that the binding of ACP to host cell GAG leads to internalization of GBS, whereas the binding of ACP to a host cell co-receptor or alternate receptor, such as integrin, leads to transcytosis of GBS, perhaps through changes in epithelial cell junctions. The possible involvement of a co-receptor for ACP on the host cell surface is compatible with the structural studies of NtACP that reveal a possible integrin-binding region in addition to the GAG-binding region (9).

Alternatively these data may indicate that binding of ACP to different GAG receptors, or to the same GAG receptor but with different affinity, may lead to different outcomes in interactions with host cells. For example, the R185A point mutation in BR2 may allow a lower affinity interaction with host cell GAG than that with the wild-type ACP; this lower affinity binding could promote transcytosis-related signaling but not internalization-related signaling; that is, signaling leading to internalization may require a higher affinity GAG-binding interaction than that leading to transcytosis. The BR2 mutation also might promote preferential binding of ACP to an alternative GAG or non-GAG host cell receptor that does not mediate internalization.

Our data, therefore, suggest that host cell entry and transcytosis by GBS may be distinct processes. The ability of our mutant strain to transcytose similarly to wild-type GBS despite reduced cell entry suggests that transcytosis may be independent of host cell internalization and possibly that transcytosis occurs primarily by a paracellular rather than an intracellular route. Similar findings, a defect in internalization but not in transcytosis, have been associated with an acapsular GBS strain, further supporting the hypothesis that internalization and transcytosis represent distinct processes (6). Paracellular transcytosis has been observed for GBS (6) and other organisms, including group A *Streptococcus* (5) and *Yersinia* sp. In particular, integrin-binding proteins of *Yersinia* sp. perturb epithelial barriers and facilitate paracellular movement of proteins and bacteria (45), supporting the possibility that ACP binds to integrin and similarly promotes its own paracellular translocation.

In summary, our data, correlating structural and functional studies of the BR2 region of ACP, support the hypotheses that this region confers the GAG-binding activity of ACP and mediates internalization of GBS by human epithelial cells. We found that a single amino acid substitution (arginine to alanine at site 185) in this GBS surface protein changes the interaction of GBS with human cells. Specifically, this mutation interferes with GBS entry into host cells but not transcytosis of these cells.

Alpha C Protein Glycosaminoglycan Binding and Cell Entry

ACP-mediated transcytosis may occur through interaction with a non-GAG host receptor, or through an interaction with host cell GAG of lower affinity than required for internalization, via paracellular movement. These data suggest that interference with the binding of ACP to its host cell receptor(s) might prevent GBS internalization and/or lethal infection. Further studies are needed to better characterize the effects of additional BR2 mutations that might eliminate GAG binding more effectively, to determine the post-receptor-binding events *in vitro* and *in vivo*, and to explore the role of the repeat regions of ACP in pathogenesis.

Acknowledgments—We thank Meghan Gilmore, Dr. Antonio Iglesias, Huong Ung, Dr. Gilles Bolduc, Dr. Karen Puopolo, Dr. David Klinzing, Dr. Lei Hua, Dr. Michael Cieslewicz, Derek Yesucevitz, Sandra L. Wong, Hope E. Hamrick, Dr. Thierry Auperin, Dr. Vincent Carey, Dr. Susan Huang, Dr. Thomas Sandora, and Dr. Elliott Kieff for discussions, advice, and technical assistance.

REFERENCES

1. Madoff, L. C., Michel, J. L., and Kasper, D. L. (1991) *Infect. Immun.* **59**, 204–210
2. Madoff, L. C., Michel, J. L., Gong, E. W., Kling, D. E., and Kasper, D. L. (1996) *Proc. Natl. Acad. Sci. U. S. A.* **93**, 4131–4136
3. Li, J., Kasper, D. L., Ausubel, F. M., Rosner, B., and Michel, J. L. (1997) *Proc. Natl. Acad. Sci. U. S. A.* **94**, 13251–13256
4. Bolduc, G. R., Baron, M. J., Gravekamp, C., Lachenauer, C. S., and Madoff, L. C. (2002) *Cell Microbiol.* **4**, 751–758
5. Cywes, C., and Wessels, M. R. (2001) *Nature* **414**, 648–652
6. Soriani, M., Santi, I., Taddei, A., Rappuoli, R., Grandi, G., and Telford, J. (2006) *J. Infect. Dis.* **193**, 241–250
7. Pier, G. B., Grout, M., and Zaidi, T. S. (1997) *Proc. Natl. Acad. Sci. U. S. A.* **94**, 12088–12093
8. Baron, M., Bolduc, G., Goldberg, M., Auperin, T., and Madoff, L. (2004) *J. Biol. Chem.* **279**, 24714–24723
9. Auperin, T. C., Bolduc, G. R., Baron, M. J., Heroux, A., Filman, D. J., Madoff, L. C., and Hogle, J. M. (2005) *J. Biol. Chem.* **280**, 18245–18252
10. Lancefield, R. C., McCarty, M., and Everly, W. N. (1975) *J. Exp. Med.* **142**, 165–179
11. Michel, J. L., Madoff, L. C., Olson, K., Kling, D. E., Kasper, D. L., and Ausubel, F. M. (1992) *Proc. Natl. Acad. Sci. U. S. A.* **89**, 10060–10064
12. Kling, D. E., Gravekamp, C., Madoff, L. C., and Michel, J. L. (1997) *Infect. Immun.* **65**, 1462–1467
13. Gravekamp, C., Horensky, D. S., Michel, J. L., and Madoff, L. C. (1996) *Infect. Immun.* **64**, 3576–3583
14. Paoletti, L. C., Ross, R. A., and Johnson, K. D. (1996) *Infect. Immun.* **64**, 1220–1226
15. Perez-Casal, J., Price, J., Maguin, E., and Scott, J. (1993) *Mol. Microbiol.* **8**, 809–819
16. Sambrook, J., Fritsch, E. F., and Maniatis, T. (1989) *Molecular Cloning: A Laboratory Manual, 2nd Ed.*, Cold Spring Harbor Laboratory Press, Cold Spring Harbor, NY
17. Caparon, M., and Scott, J. (1991) *Methods Enzymol.* **204**, 556–586
18. Alberti, S., Ashbaugh, C. D., and Wessels, M. R. (1998) *Mol. Microbiol.* **28**, 343–353
19. Otwinowski, Z., and Minor, W. (1997) *Methods Enzymol.* **276**, 307–326
20. Collaborative Computational Project, N. (1994) *Acta Crystallogr. Sect. D Biol. Crystallogr.* **50**, 760–763
21. Vagin, A., and Teplyakov, A. (1997) *J. Appl. Crystallogr.* **30**, 1022–1025
22. Murshudov, G. N., Vagin, A. A., and Dodson, E. J. (1997) *Acta Crystallogr. Sect. D Biol. Crystallogr.* **53**, 240–255
23. Emsley, P., and Cowtan, K. (2004) *Acta Crystallogr. Sect. D Biol. Crystallogr.* **60**, 2126–2132
24. Schomaker, V., and Trueblood, K. N. (1968) *Acta Crystallogr. Sect. B Struct. Crystallogr. Cryst. Chem.* **24**, 63–76
25. Cieslewicz, M., Kasper, D. L., Wang, Y., and Wessels, M. (2001) *J. Biol. Chem.* **276**, 139–146
26. Carter, W., Cama, E., and Huntington, J. (2005) *J. Biol. Chem.* **280**, 2745–2749
27. Faham, S., Hileman, R., Fromm, J., Linhardt, R., and Rees, D. (1996) *Science* **271**, 1116–1120
28. Pinheiro, J., and Bates, D. (2000) *Mixed-effects Models in s and s-plus*, pp. 1–52, Springer Verlag, Heidelberg
29. Tamura, G. S., Kuypers, J. M., Smith, S., Raff, H., and Rubens, C. E. (1994) *Infect. Immun.* **62**, 2450–2458
30. Teti, G., Tomasello, F., Chiofalo, M. S., Orefici, G., and Mastroeni, P. (1987) *Infect. Immun.* **55**, 3057–3064
31. Doran, K. S., Chang, J. C., Benoit, V. M., Eckmann, L., and Nizet, V. (2002) *J. Infect. Dis.* **185**, 196–203
32. Adderson, E., Takahashi, S., Wang, Y., Armstrong, J., Miller, D., and Bohnsack, J. (2003) *Infect. Immun.* **71**, 6857–6863
33. Schubert, A., Zakikhany, K., Pietrocola, G., Meinke, A., Speziale, P., Eikmanns, B., and Reinscheid, D. (2004) *Infect. Immun.* **72**, 6197–6205
34. Gutekunst, H., Eikmanns, B., and Reinscheid, D. (2004) *Infect. Immun.* **72**, 3495–3504
35. Cheng, Q., Debol, S., Lam, H., Eby, R., Edwards, L., Matsuka, Y., Olmsted, S. B., and Cleary, P. P. (2002) *Infect. Immun.* **70**, 6409–6415
36. Dramsi, S., Caliot, E., Bonne, I., Guadagnini, S., Prevost, M., Kojadinovic, M., Lalioui, L., Poyart, C., and Trieu-Cuot, P. (2006) *Mol. Microbiol.* **60**, 1401–1413
37. Brown, C., Gu, Z., Matsuka, Y., Purushothaman, S., Winter, L., Cleary, P., Olmsted, S., Ohlendorf, D., and Earhart, C. (2005) *Proc. Natl. Acad. Sci. U. S. A.* **102**, 18391–18396
38. Fischer, J., LeBlanc, K., and Leong, J. (2006) *Infect. Immun.* **74**, 435–441
39. Putten, J. v., Duensing, T., and Cole, R. (1998) *Mol. Microbiol.* **29**, 369–379
40. Henry-Stanley, M., Hess, D., Erlandsen, S., and Wells, C. (2005) *Shock* **24**, 571–576
41. Patrie, K., Botelho, M., Franklin, K., and Chiu, I. (1999) *Biochemistry* **38**, 9264–9272
42. Fry, E., Lea, S., Jackson, T., Newman, J., Ellard, F., Blakemore, W., Abughazaleh, R., Samuel, A., King, A., and Stuart, D. (1999) *EMBO J.* **18**, 543–554
43. Gao, R., and Brigstock, D. (2004) *J. Biol. Chem.* **279**, 8848–8855
44. Summerford, C., Bartlett, J. S., and Samulski, R. J. (1999) *Nat. Med.* **5**, 78–82
45. Tafazoli, F., Homstrom, A., Forsberg, A., and Magnusson, K. (2000) *Infect. Immun.* **68**, 5335–5343
46. Nicholls, A., Sharp, K. A., and Honig, B. (1991) *Proteins* **11**, 281–296

Identification of a Glycosaminoglycan Binding Region of the Alpha C Protein That Mediates Entry of Group B *Streptococci* into Host Cells

Miriam J. Baron, David J. Filman, Gina A. Prophete, James M. Hogle and Lawrence C. Madoff

J. Biol. Chem. 2007, 282:10526-10536.

doi: 10.1074/jbc.M608279200 originally published online January 26, 2007

Access the most updated version of this article at doi: [10.1074/jbc.M608279200](https://doi.org/10.1074/jbc.M608279200)

Alerts:

- [When this article is cited](#)
- [When a correction for this article is posted](#)

[Click here](#) to choose from all of JBC's e-mail alerts

This article cites 44 references, 25 of which can be accessed free at <http://www.jbc.org/content/282/14/10526.full.html#ref-list-1>